

The Extralemniscal System Modulates Early Somatosensory Cortical Processing

Sofija Perovic,^{1,2}  Richard Somervail,^{1,3,4}  Diego Benusiglio,^{1,5} and  Gian Domenico Iannetti^{1,4}

¹Neuroscience and Behaviour Laboratory, Italian Institute of Technology (IIT), Rome 00161, Italy, ²Department of Physiology and Pharmacology, University of Rome, Sapienza, Rome 00185, Italy, ³Translational and Computational Neuroscience Unit, Manchester Metropolitan University, Manchester M15 6GX, United Kingdom, ⁴Department of Neuroscience, Physiology and Pharmacology, University College London (UCL), London WC1E 6BT, United Kingdom, and ⁵European Molecular Biology Laboratory (EMBL), Epigenetics and Neurobiology Unit, Rome 00015, Italy

Sudden and surprising sensory changes signal environmental events that may require immediate behavioral reactions. In mammals, these changes engage nonspecific “extralemniscal” thalamocortical pathways and evoke large and widespread cortical vertex potentials (VPs). Extralemniscal activity modulates cortical motor output in a variety of tasks and facilitates purposeful and immediate behavioral responses. In contrast, whether the extralemniscal system also affects cortical processing of sensory input transmitted through canonical “lemniscal” thalamocortical pathways remains unknown. Here we tested this hypothesis. In 23 healthy human participants (11 females) we continuously probed lemniscal processing in the primary somatosensory cortex (S1) by measuring the early-latency evoked potentials elicited by a stream of high-frequency (9.5 Hz) somatosensory electrical stimuli. We concurrently recorded extralemniscal activity by measuring the large VP elicited by fast-rising and infrequent (~ 0.1 Hz) auditory pure tones. We observed that the amplitude of S1 responses changes as a function of the phase of the VP, an effect consequent to a modulation of lemniscal input at the cortical rather than subcortical level. These findings demonstrate that a transient activation of the extralemniscal system interferes with ongoing cortical functions across different brain systems—i.e., not only at the level of the motor output but already at the sensory input—and thereby influences global brain dynamics.

Key words: electroencephalography (EEG); global brain dynamics; somatosensory-evoked potentials (SEP); surprise; thalamocortical pathways; vertex potential

Significance Statement

Abrupt and surprising stimuli signaling environmental events requiring immediate behavioral reactions engage the nonspecific “extralemniscal” sensory system and elicit some of the largest brain responses in mammals. These responses modulate cortical output in preparation for swift and appropriate behaviors. However, it remains unclear whether a sudden activation of the extralemniscal system by surprising stimuli affects not only motor output but also the first cortical handling of sensory input. Here we show that the extralemniscal system interferes already with the earliest stages of sensory processing in primary sensory cortices. Thus, the extralemniscal system affects ongoing cortical functions across different brain systems and thereby influences global brain dynamics.

Introduction

Despite the unity of perception (Peacocke, 2015), mammals sense the world through two fundamentally distinct sensory

systems, each with its segregated ascending pathways (Albe-Fessard and Besson, 1973; Mountcastle, 1974; Hu, 2003; Somervail et al., 2025).

Canonical lemniscal (or specific) sensory systems project in an orderly topographic manner to modality-specific thalamic nuclei and cortical areas and transmit information about sensory stimuli with high fidelity (Mountcastle, 1974). For example, the somatosensory lemniscal system has precise somatotopy and frequency specificity even when stimuli are repeated at high frequency (Albe-Fessard and Besson, 1973; Mountcastle, 2005; Lemus et al., 2010).

Conversely, the extralemniscal (or nonspecific) sensory system transmits information about the occurrence of sudden and surprising environmental changes that potentially require immediate behavioral reactions. The extralemniscal system is engaged by

Received Sept. 9, 2024; revised July 22, 2025; accepted Aug. 1, 2025.

Author contributions: S.P., R.S., and G.D.I. designed research; S.P. performed research; S.P., R.S., and G.D.I. analyzed data; S.P., R.S., D.B., and G.D.I. wrote the paper.

We thank Drs. Santiago Rompani and André Mouraux, as well as all lab members for their excellent comments on earlier versions of this manuscript. This work was supported by Istituto Italiano di Tecnologia (IIT) and European Molecular Biology Laboratory (EMBL).

The authors declare no competing financial interests.

Correspondence should be addressed to Gian Domenico Iannetti at g.iannetti@ud.ac.uk, giandomenico.iannetti@gmail.com.

This paper contains supplemental material available at: <https://doi.org/10.1523/JNEUROSCI.1815-24.2025>
<https://doi.org/10.1523/JNEUROSCI.1815-24.2025>

Copyright © 2025 the authors

stimuli of multiple sensory modalities (Albe-Fessard and Besson, 1973; Komura et al., 2005) provided that they are fast-rising and delivered at long and variable intervals. Indeed, this system's activity rapidly habituates when stimuli are repeated at 1 Hz or more, i.e., when they become predictable (Albe-Fessard and Rougeul, 1958; Iannetti et al., 2008). Once engaged, the extralemniscal system modulates the overall arousal level and global cortical activity through the reticular formation and the nonspecific thalamic nuclei (Moruzzi and Magoun, 1949; Abrahamian et al., 1963).

These rules of engagement are informative about the functional significance of the transient electrocortical responses elicited by abrupt sensory stimuli. It is well accepted that stimuli presented at high frequency (e.g., somatosensory stimulation of the median nerve at 5–10 Hz) engage the lemniscal system and elicit small-amplitude and short-latency cortical responses in the pertinent primary sensory cortex. The most notable short-latency somatosensory evoked potentials (SEPs) are the N20–P25 complex and the P45 wave, which respectively reflect the first arrival of the lemniscal input to the cortex and later intracortical processing within a larger neuronal population (Desmedt et al., 1983; Desmedt and Bourguet, 1985; Nuwer et al., 1994; Baker et al., 2003; Crucu et al., 2008). These early waves occur within 50 ms from the onset of median nerve stimulation and have amplitudes usually smaller than 1 μ V.

In contrast, abrupt stimuli of any sensory modality presented at long and variable intervals (e.g., 5–20 s) elicit large-amplitude, long-latency, and widespread potentials (Davis et al., 1939; Bancaud et al., 1953; Gastaut et al., 1954; Mouraux and Iannetti, 2009) that likely reflect the engagement of the extralemniscal system (Albe-Fessard and Besson, 1973; Somervail et al., 2021, 2022, 2025). These potentials consist in a biphasic, negative-positive complex, lasting up to 500 ms after the stimulus onset and with peak-to-peak amplitudes that can be larger than 100 μ V in single trials (Fig. 1). Rather than being localized in primary sensory cortices, their topography is widespread and symmetrically distributed, with maximal amplitude at the scalp vertex (Cz) and for this reason they are referred to as vertex potentials (VPs; Bancaud et al., 1953; Gastaut et al., 1954; Clynes, 1969).

The occurrence of a VP affects cortical output in a variety of motor tasks. This makes intuitive sense given that the extralemniscal system is sensitive to environmental changes that potentially require fast behavioral reactions. For example, VP amplitude is tightly coupled, both within and across subjects, with a transient disruption of the corticospinal drive mediating both isometric force and high-precision kinematic tasks, in the form of a biphasic pattern consisting in a first inhibition followed by an enhancement (Novembre et al., 2018, 2024; Somervail et al., 2022; see also Novembre and Iannetti, 2021). A similar biphasic pattern of disruption of motor output concomitant to a VP is observed in the frequency of both saccades and microsaccades (Engbert and Kliegl, 2003; Kerzel et al., 2010).

In contrast to this clear modulation of cortical output, whether the extralemniscal system also affects cortical processing of sensory input transmitted through canonical thalamocortical pathways remains unknown. Here we tested the hypothesis that the disruption of ongoing cortical processing is a general phenomenon, by probing whether lemniscal thalamocortical processing is modulated by a transient activation of the extralemniscal system.

Materials and Methods

Participants

Twenty-three healthy human participants [11 females, age 28 ± 5 years (mean \pm SD), age range 21–45 years] took part in the experiment. All

participants gave written consent before taking part in the study. Procedures were approved by the local ethical committee.

Experimental design

Experiments took place in a dim, quiet, and temperature-controlled room. Participants were seated, with the stimulated arm resting comfortably on a table. During data acquisition, they were required to keep their gaze on a fixation cross (4×4 cm) placed centrally in front of them, at a distance of ~ 50 cm, 30° below the eye level. They received a continuous stream of somatosensory stimuli and, at the same time, a smaller number of isolated auditory stimuli (Fig. 1). The experiment consisted of 12 successive blocks, each lasting ~ 5 min. Each block comprised 40 auditory stimuli and $\sim 3,138$ (range 3,003–3,274) somatosensory stimuli. The interval between consecutive blocks was ~ 2 min.

Sensory stimuli

Auditory stimuli were brief and fast-rising tones (60 ms duration, 15 ms rise and fall times, frequency 800 Hz) presented at a loud but comfortable level (~ 80 dB), delivered through a loudspeaker placed on the participant's left side. Auditory stimuli were delivered with an interstimulus interval of 6–10 s (uniform distribution). Somatosensory stimuli were constant-current biphasic square-wave electrical pulses (200 μ s duration; DS8R, Digitimer) delivered using a surface bipolar electrode (0.5 cm diameter, 3 cm interelectrode distance) placed over the median nerve at the left wrist. The intensity of somatosensory stimulation was initially adjusted in each participant to elicit a reproducible thumb muscle twitch, and then, during the data acquisition, delivered 10% above this motor threshold. Somatosensory stimuli were delivered continuously at 9.5 Hz.

EEG recording and preprocessing

The electroencephalogram (EEG) was recorded using 64 active electrodes placed on the scalp according to the international 10–10 system. EEG signals were amplified and digitized using a sampling rate of 8,192 Hz (Biosemi Active-2 system) and preprocessed and analyzed using MATLAB (version 2021a, MathWorks) and Letswave (Mouraux and Iannetti, 2008). Continuous EEG data were first rereferenced to the average of the earlobes and bandpass filtered 0.5–2,000 Hz and then segmented into 2-s-long epochs relative to the onset of each auditory stimulus (-1 to $+1$ s). Epochs with amplitude values exceeding ± 100 μ V in one or more electrodes (i.e., epochs probably contaminated by artifacts) were rejected. These epochs constituted $2.8 \pm 2.2\%$ of the total number of epochs. Artifacts due to blinks, eye movements, muscle movements, and auditory stimulation were removed using a validated method based on independent component analysis (ICA; Jung et al., 2000). Following this basic preprocessing, epochs were further processed in three separate pipelines for (1) responses to auditory stimuli, (2) responses to somatosensory stimuli delivered during auditory stimulation, and (3) responses to somatosensory stimuli delivered without concomitant auditory stimulation, as follows.

VP processing (“VP-epochs”). To identify the auditory-evoked VP, epochs underwent two additional processing steps. First, they were low-pass filtered at 30 Hz. Second, we assessed whether, in each epoch, there were electrodes whose amplitude did not correlate with the average of their neighboring electrodes (Pearson's $r > 0.5$). If that was the case, these electrodes were interpolated using the average signal from their neighboring electrodes. If >6 electrodes needed interpolation, the entire epoch was rejected, and if $>10\%$ of epochs were rejected, this criterion was raised to 10 electrodes to prevent excessive data loss (this occurred only in one participant). The number of rejected “VP-epochs” was $0.17 \pm 0.35\%$ of the total number of epochs. Single-subject average waveforms of “VP-epochs” were computed for each participant.

SEP processing (“SEP-epochs”). To identify early-latency SEPs, each 2-s-long epoch segmented relative to the onset of the auditory stimulus was further segmented relative to the onset of each somatosensory stimulus (-20 to 100 ms) and bandpass filtered 30–300 Hz. In these “SEP-epochs,” a second ICA was performed to remove the electrical stimulation artifact. After ICA, we used the same criteria applied to “VP-epochs” to reject epochs. The number of rejected “SEP-epochs”

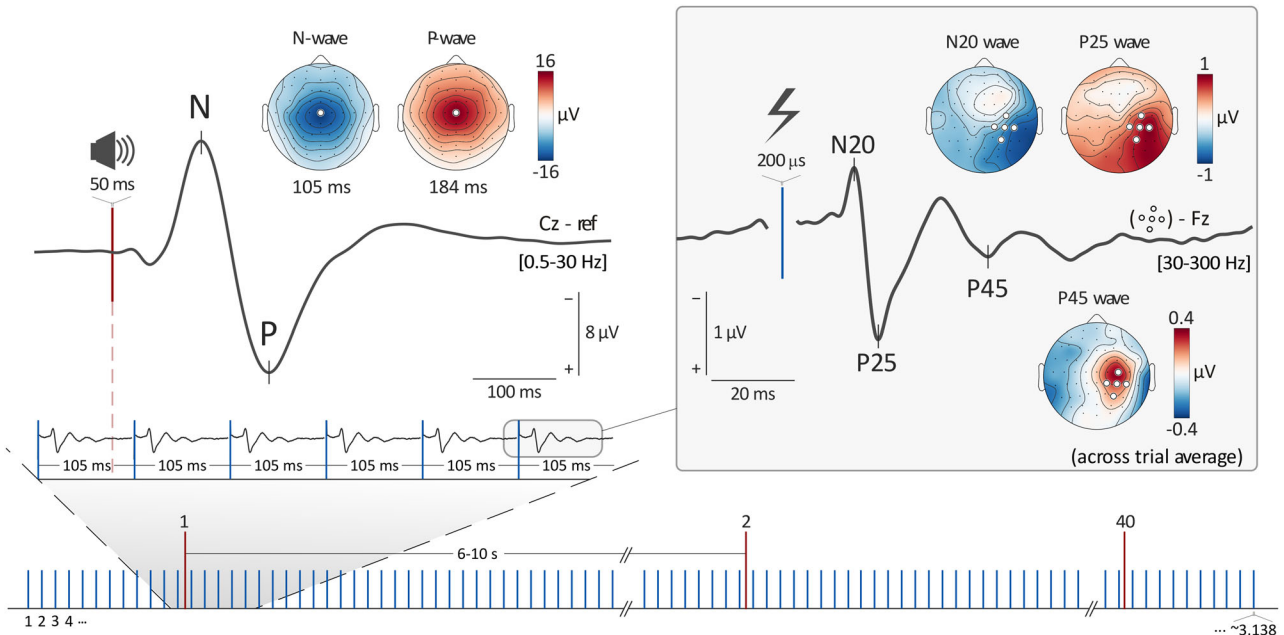


Figure 1. Experimental design. Bottom, In each experimental block participants received a stream of $\sim 3,138$ somatosensory stimuli (blue), consisting in brief electrical pulses delivered transcutaneously at 9.5 Hz to the left median nerve at the wrist. Throughout the somatosensory stimulation, 40 loud and fast-rising auditory stimuli (red) were delivered every 6–10 s through a loudspeaker placed in front of the participant’s left hand. Top left, Each auditory stimulus elicited a large-amplitude VP in the ongoing 64-channel EEG, consisting in a centrally distributed negative–positive deflection maximal at the vertex (Cz, highlighted in white in the scalpmaps). Top right, Electrical stimuli elicited early SEPs consisting of three main peaks (N20, P25, and P45) maximal over the somatosensory cortex contralateral to the stimulated hand (electrodes highlighted in white in the scalpmaps). Note the smaller amplitude and higher frequency of SEPs compared with the VP. In subsequent analyses we assessed whether the amplitude of early SEPs depended on where they occurred with respect to the phase of the concomitant VP.

was $0.67 \pm 0.96\%$. Finally, “SEP-epochs” were rereferenced to Fz (Nuwer et al., 1994) and baseline corrected using the -20 to -10 ms prestimulus interval. Bandpass filtering and baseline correction of “SEP-epochs” ensured that the VP did not exert a trivial additive effect on the SEP waveforms (Fig. 2).

Control SEP processing (“control SEP-epochs”). To control for possible effects of the spontaneous EEG activity on early SEPs, we segmented EEG periods devoid of auditory stimulation into 2-s-long epochs centered around 40 dummy auditory stimuli located at equal distance from the preceding and following real auditory stimuli. Given that the ISI between auditory stimuli ranged between 6 and 10 s, the dummy stimuli occurred at least 3 s before or after the real auditory stimuli. We refer to these epochs as “control SEPs-epochs.” These data underwent the same processing described for “VP-epochs” and “SEP-epochs.”

EEG analysis

SEP binning relative to the phase of the average VP (“average-VP phase binning”). We wanted to test whether SEP amplitude depended on the phase of the concomitant VP. To this end, we assigned each single-trial “SEP-epoch” (on the basis of the onset of its somatosensory stimulus) occurring within 300 ms from the onset of the auditory stimulus to one of the six 50-ms-long consecutive time bins covering the VP as follows: #1, 0–50 ms (before the VP); #2, 50–100 ms (first half of the N wave); #3, 100–150 ms (second half of the N wave); #4, 150–200 ms (beginning of the P wave); #5, 200–250 ms (second part of the P wave); and #6, 250–300 ms (after the VP; Fig. 3, left panel). We then averaged the SEP responses evoked by the somatosensory stimuli within each of the six time bins described above and obtained, for each subject, six average SEP waveforms. Table 1 shows the number of single-trial SEPs for each participant and for each time bin: across participants, the number of single trials in each bin was highly similar, ranging between 212 and 223.

To test whether the SEP amplitude depended on the VP phase, we performed a repeated-measure point-by-point one-way ANOVA, with six levels (bins #1–6). To account for multiple comparisons across time points and EEG electrodes, we used cluster-based permutation

testing (Maris and Oostenveld, 2007). Therefore, clusters were based on both temporal consecutivity and spatial adjacency of EEG electrodes with ANOVA p values of <0.05 . Spatial adjacency was based on electrode distance and set so that each electrode had, on average, six neighbors. Once these clusters were identified, permutation testing was used to assess their significance. Specifically, the data were permuted 1,000 times by randomly reassigning condition labels (bins #1–6) across the subject-level averages within each subject, to generate a null distribution of chance-level summed cluster F values. This null distribution was used to define a threshold ($p = 0.05$) against which the summed F values of the clusters from the actual data were assessed. Thus, only the clusters surviving both thresholds (consecutivity in time and adjacency in space, as well as random permutations) were considered significant. Finally, given the difficulty of interpreting ANOVA F statistics, we performed post hoc t tests (one-tailed) between all possible bin pairs to explore directional differences. To account for multiple comparisons, we performed separate cluster-based permutation testing on the outcome of each post hoc comparison.

SEP binning relative to the phase of single-trial VPs (“single-trial VP phase binning”). To test whether the SEP modulation truly depended on the VP phase, we exploited the large signal-to-noise ratio of auditory VPs (e.g., Fig. 2 in Kilintari et al., 2018) and their variability in latency, both across subjects and across trials (Mouraux and Iannetti, 2008; Hu et al., 2011). We estimated the single-trial latency of the negative and positive peaks of each single-trial VP, as follows. We first used each participant’s average-VP waveform at Cz to define two 80-ms-long time intervals, encompassing the peaks of the N wave and of the P wave. Within these two time windows, we extracted, for each single trial, the latency of the most negative and most positive time point, respectively. We then used these single-trial N and P latencies to bin each individual SEP (again on the basis of the onset of its somatosensory stimulus) as a function of the phase of the concomitant single-trial VP, according to the following procedure (Fig. 3, right panel). We first defined bins #3 and #5, which consisted of a 50 ms time interval centered around the N and P peak, respectively. Subsequently, we defined the remaining bins relative to bins #3 and #5, as follows. Bins #1 and #2 were two 50 ms time

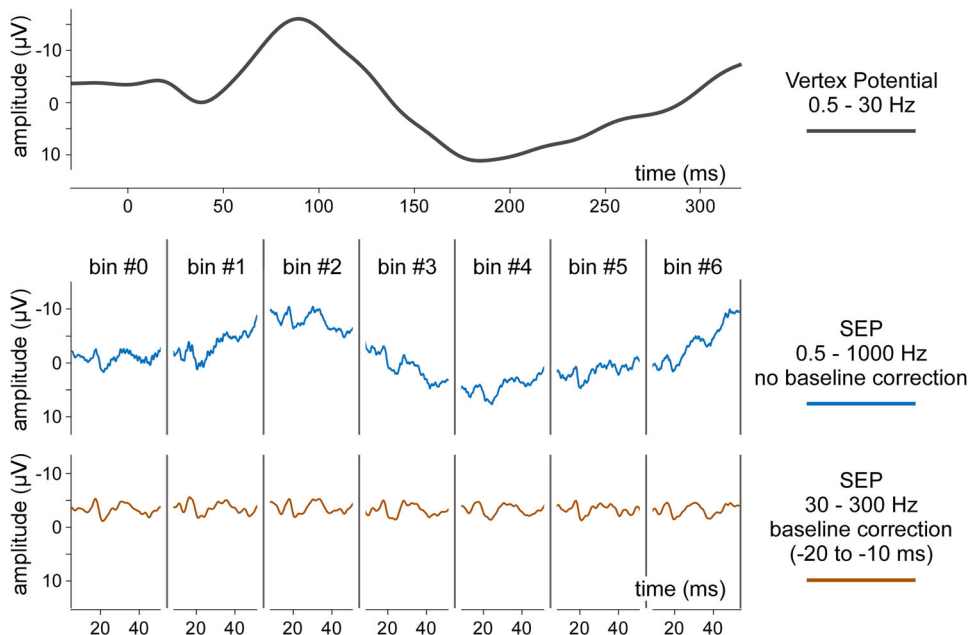


Figure 2. Lack of evidence of a trivial additive effect of the VP on the SEP waveform. Top panel, Across-trial average waveform of the auditory-evoked VP from a representative subject (channel Cz, bandpass filtered 0.5–30 Hz). Middle panel, Average SEP waveforms were obtained by grouping single-trial SEPs in seven time bins covering the entire length of the concomitant VP (see Materials and Methods for details). These SEP-epochs (blue) were neither high-pass filtered nor baseline corrected. Note how the large deflections of the concomitant VP add to the amplitude of the SEP waveforms. Bottom panel, Same binned SEP averages but with SEP-epochs (red) bandpass filtered 30–300 Hz and baseline corrected (from −20 to −10 ms with respect to the stimulus onset). Note how this preprocessing step removes the additive effect shown in the middle panel. Bandpass filtering at 30–300 Hz and baseline correction were applied to all SEP data reported in this manuscript.

intervals preceding bin #3. Bin #6 was a 50 ms time interval following bin #5. Bin #4 had a variable duration, contingent on the time interval between the end of bin #3 (N peak) and the onset of bin #5 (P peak) and thus corresponded to the transition between N and P. The average length of bin #4 was 40 ± 29 ms. In $5.5 \pm 3.9\%$ of single trials, in which the N–P interpeak interval was <50 ms, there was no bin #4. To test whether the SEP amplitude depended on the specific phase of each “single-trial” VP, we performed a repeated-measure point-by-point one-way ANOVA, with six levels (bins #1–6). As described above, to account for multiple comparisons across time points and EEG electrodes, we used cluster-based permutation testing (Maris and Oostenveld, 2007). Again, to interpret ANOVA results, we performed post hoc *t* test comparisons, with cluster correction.

Control SEP binning relative to the phase of spontaneous EEG deflections (“dummy VP phase binning”). The single-trial latency estimation used in the previous analysis selects the most negative and positive time points in the two time windows containing the N and P peaks in the across-trial average VP. Thus, this approach always highlights one local minimum and one local maximum, even in the absence of a VP, which potentially creates the confound of selecting negative and positive deflections of the spontaneous EEG (for a discussion about this, see Hu et al., 2010, 2011). To address this issue and ascertain whether SEPs were truly modulated by the phase of single-trial VPs, we grouped single-trial control SEPs in six time bins defined using a procedure identical to that performed for the “single-trial VP phase binning” but applied to EEG periods devoid of auditory stimulation. We then performed the same repeated-measure point-by-point one-way ANOVA, with six levels (bins #1–6; Fig. S1).

P45 modulation timocourse. To understand how the P45 modulation unfolded over time, we took the SEP waveforms obtained in the “single-trial VP phase binning” analysis and extracted the P45 amplitude in each subject and time bin. The P45 amplitude was defined as the mean voltage in a 42–45 ms time window from the cluster of electrodes overlying the contralateral S1 (i.e., where the P45 was maximal: P2, P4, P6, CP4, PO4). To quantify the change in P45 amplitude, we used the P45 amplitude in

the absence of the VP (bin #1 from “dummy VP phase binning”) as the baseline. To test the P45 modulation as a function of single-trial VP phase, we performed a one-way ANOVA (six levels: bins #1–6). Given the hypothesis that the N and P waves reflect opposite changes of cortical excitability, we performed two post hoc analyses comparing bin #2 with bin #4 and bin #2 and bin #5. The choice of these bins was made considering in which bin the P45, rather than the stimulus onset, occurred—so that bins #2 and #4 corresponded to the N peak and P peak of the VP, respectively.

To ascertain that the P45 modulation was conditional to the presence of the VP, we performed the same analysis on the P45 amplitude extracted from the “control SEP-epochs” (i.e., the epochs obtained through the “dummy VP phase binning”).

Robustness of the chosen P45 time window. To test whether the P45 modulation depended on the time interval chosen to extract the P45 amplitude (42–45 ms), we also extracted the P45 amplitudes from three additional, wider time windows: 44–48 ms (4 ms wide), 42–48 ms (6 ms wide), and 40–50 ms (10 ms wide; Fig. S2). The use of wider time windows has the advantage of including the P45 component in participants with short and long peak latencies, but the disadvantage of diluting possible effects due to the inclusion of time points before and after the P45 component.

Selectivity of P45 modulation. To further explore the selectivity of the P45 modulation, we repeated the timocourse analysis on two additional time intervals, one in the prestimulus (−15 to −10 ms) and one at the end of the epoch (50–54 ms; Fig. S3).

Results

EEG waveforms and topographies

Auditory-evoked VP

Isolated auditory stimuli delivered at long and variable interstimulus interval elicited a typical large VP (peak-to-peak amplitude, 30 ± 10 μ V; participant-level mean \pm SD). Both the N and P waves were symmetrically distributed, with maximal amplitude

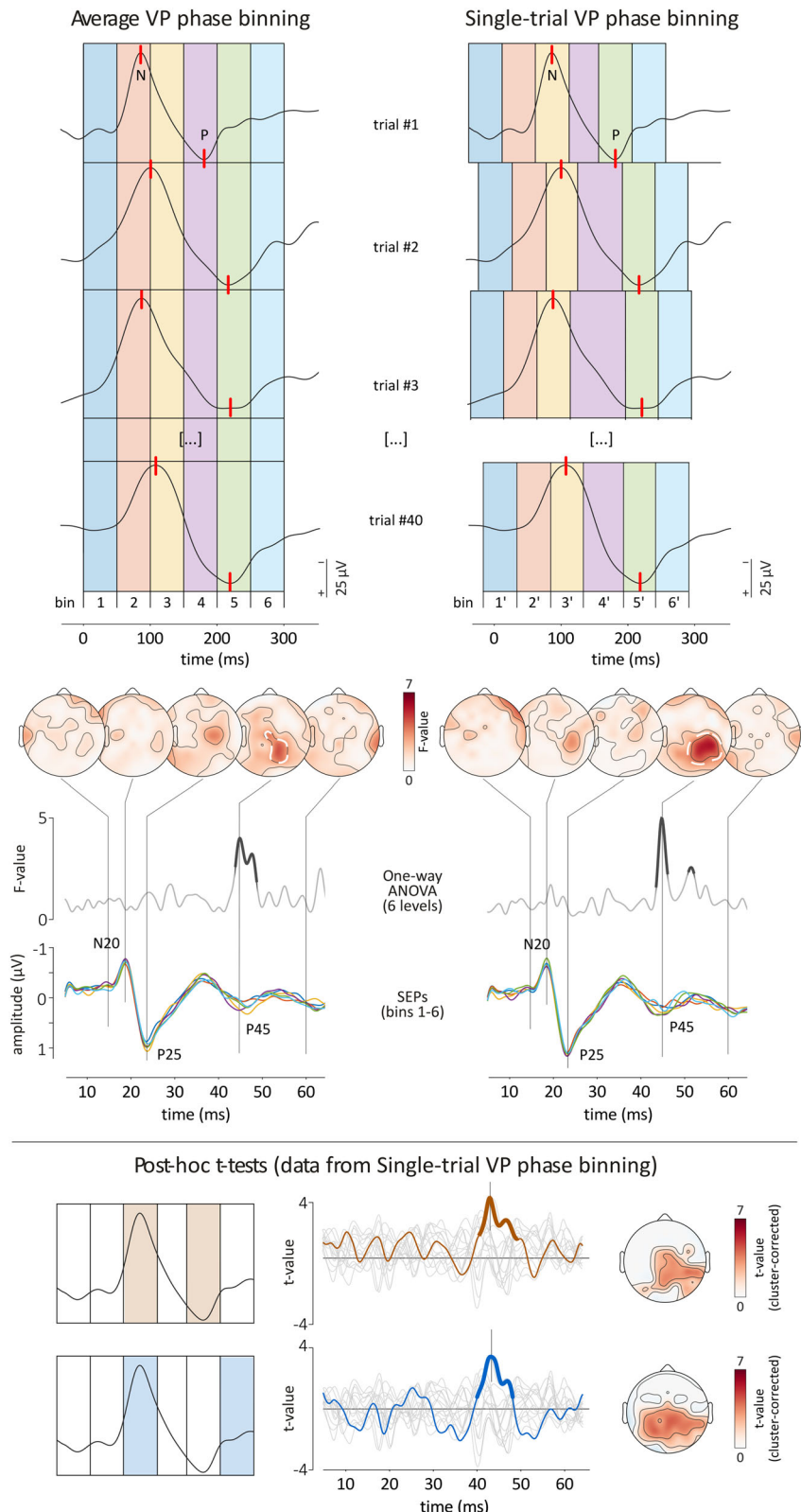


Figure 3. The modulation of S1 responses to lemniscal input is tightly coupled to the occurrence of single-trial VPs. Top panel, In the “average-VP phase binning” (left column), we grouped somatosensory stimuli in six bins with respect to when they occurred in relation to the phase of the group-level VP average waveform at Cz, as follows: bin #1, 0–50 ms; bin #2, 50–100 ms; bin #3, 100–150 ms; bin #4, 150–200 ms; bin #5, 200–250 ms; and bin #6, 250–300 ms. In the “single-trial VP phase binning” (right column), we binned each individual SEP as a function of the single-trial latency of the N and P waves of each single-trial VP at Cz, as follows. We first identified the N and P peak latencies and defined two 50-ms-long bins, each centered around a peak (bins #3' and #5', respectively). We then defined two 50 ms bins preceding the N peak (bin #1' and bin #2') and one 50 ms bin following the P peak (bin #6'). We finally defined a bin of variable duration (bin #4') between bins #3' and #5'. After such phase-dependent binning, we calculated, for each participant, the average SEP elicited by somatosensory stimuli occurring in each bin. A point-by-point ANOVA (six levels, bins #1–6 or 1'–6') on the resulting SEPs revealed a cluster of across-bin modulation located on the contralateral somatosensory cortex at the latency of the P45 component [“average-VP phase binning”: a maximum F value at 44 ms poststimulus ($F_{(5,17)} = 3.95$; $p = 0.0024$; channel P4); and a significant space-time cluster ($F_{(5,17)} = 2,292.21$;

Table 1. Number of single-trial SEPs for each participant (rows) and time bin (columns)

Participant	Bin #1	Bin #2	Bin #3	Bin #4	Bin #5	Bin #6	Mean	SD
1	220	208	234	209	236	207	219	13.3
2	214	199	209	222	211	219	212.3	8.1
3	201	208	207	217	213	208	209	5.5
4	215	220	218	222	219	227	220.2	4.1
5	237	214	232	229	226	224	227	7.8
6	237	216	236	216	235	217	226.2	10.8
7	229	215	231	229	230	222	226	6.3
8	201	217	192	220	197	223	208.3	13.2
9	218	197	221	206	215	209	211	8.8
10	243	197	245	211	245	208	224.8	21.9
11	192	238	207	240	214	240	221.8	20.5
12	247	206	243	206	232	216	225	18.2
13	212	219	206	221	209	219	214.3	6.2
14	212	219	205	222	209	224	215.2	7.6
15	225	213	232	209	235	210	220.7	11.5
16	229	199	228	206	222	204	214.7	13.2
17	212	213	213	222	215	213	214.7	3.7
18	248	200	253	199	258	200	226.3	29.4
19	228	201	238	212	229	217	220.8	13.4
20	210	206	215	201	221	192	207.5	10.3
21	190	222	195	220	209	218	209	13.6
22	219	209	222	217	224	217	218	5.2
23	209	240	209	231	226	223	223	12.3
mean	219.5	212	221.3	216.8	223	215.5	218	4
SD	16.2	11.6	16.4	10.2	13.6	10.1	6.5	

Note how, across participants, the number of single trials in each bin was highly similar, ranging between 212 and 223. Values in bold show average number of trials across bin and participant averages (218), as well as standard deviation across participant averages (4) and across bin averages (6.5).

at the vertex (Cz). The N wave (peak latency, 102 ± 10 ms; amplitude 14 ± 6 μ V; participant-level mean \pm SD) extended bilaterally toward the temporal regions, while the P wave (peak latency, 184 ± 23 ms; amplitude 15 ± 7 μ V; participant-level mean \pm SD) had a more central distribution (Fig. 1, left panel).

Early-latency SEPs

Somatosensory stimuli delivered at 9.5 Hz over the left median nerve elicited the typical N20, P25, and P45 deflections in the ongoing EEG (Nuwer et al., 1994). Their amplitude was maximal over the electrodes corresponding to the primary somatosensory cortex (S1) contralateral to the stimulated hand (P2, P4, P6, CP4, PO4; Fig. 1, right panel). Their latency and amplitude were as follows: N20, 18 ± 2 ms, -1.0 ± 0.8 μ V; P25, 23 ± 1 ms, 1.2 ± 0.8 μ V; P45, 46 ± 4 ms, 0.5 ± 0.3 μ V; participant-level mean \pm SD).

The amplitude of S1 responses is modulated by surprising auditory stimuli

We observed a clear change in the amplitude of S1 responses when somatosensory stimuli were delivered during a concomitant auditory-evoked VP (Fig. 3, Fig. S1). Specifically, this

effect mostly occurred in the temporal and spatial interval of the P45 component. This was demonstrated by binning SEPs relative to the phase of the average VP (“average-VP phase binning”) and using single-subject-level average SEP waveforms of the six bins for a repeated-measure one-way ANOVA. This analysis revealed a maximum F value at 44 ms poststimulus ($F_{(5,17)} = 3.95$; $p = 0.0024$; channel P4) and a significant space-time cluster (cluster $F_{(5,17)} = 2,292.21$; cluster $p = 0.017$; Fig. 3, top left panel).

We also binned SEP more precisely by taking into account the trial-by-trial jitter of VP latency. This “single-trial VP phase binning” showed, again, the maximum F value at 44 ms poststimulus occurring in the spatiotemporal interval of the P45 SEP component ($F_{(5,17)} = 5.03$; $p = 0.0003$; channel P4) with a significant space-time cluster (cluster $F_{(5,17)} = 2,419.61$; cluster $p = 0.014$; Fig. 3, top right panel).

To finally verify that the SEP modulation revealed in the “single-trial VP phase binning” analysis was not confounded by the selection of local minima and maxima in the ongoing EEG, we performed the same analysis but using the control SEPs measured in periods devoid of auditory stimulation (“dummy VP phase binning”; see Materials and Methods). The same point-by-point ANOVA on these control data showed no evidence of modulation of SEP amplitude (44 ms poststimulus, $F_{(5,17)} = 1.45$; $p = 0.2116$; channel P4), and no statistically significant clusters were identified (Fig. S1).

Modulation of S1 responses is tightly coupled to the VP phase

The abovementioned data-driven analyses conducted on the entire SEP timecourse demonstrated a clear effect of the auditory-evoked VP on the response amplitude, an effect mostly occurring within the time interval and scalp location corresponding to the P45 SEP component (Fig. 3, top panel). We further explored possible directional differences across bins in two different ways: (1) by performing post hoc point-by-point t tests and (2) by extracting the timecourse of a summary metric of P45 amplitude.

- Point-by-point post hoc t tests between all possible bin pairs of the “single-trial VP phase binning” data revealed that the main effect observed in point-by-point ANOVAs was driven by the P45 component roughly occurring during the N and P waves of the VP, as the only comparisons surviving space-time cluster correction were bins #2 versus #4 (cluster $t = 2,607.76$; cluster $p = 0.040$) and #2 versus #5 (cluster $t = 2,946.37$; cluster $p = 0.032$). Specifically, SEP amplitude in the time interval corresponding to the P45 component was smaller in bin #2 compared with bins #4 and #5 (Fig. 3, bottom panel). The post hoc tests performed on the “average-VP phase binning” data also revealed that the P45 component was modulated when occurring during the N and P waves of the VP: the P45 was smaller in bin #2 compared with bin #4 (cluster $t = 2,691.56$; cluster $p = 0.025$).

←

cluster $p = 0.017$; “single-trial VP phase binning”: a maximum F value at 44 ms poststimulus ($F_{(5,17)} = 5.03$; $p = 0.0003$; channel P4); and a significant space-time cluster (cluster $F_{(5,17)} = 2,419.61$; cluster $p = 0.014$). Note that in the case of “Single-trial VP phase binning,” there are two distinct time intervals that show a cluster-level significance at channel P4, while in fact they constitute a single, continuous cluster. Bottom panel, To determine the directionality of the observed modulation, we performed point-by-point post hoc t tests between all possible bin pairs. This analysis revealed that in the “single-trial VP phase binning” data, the observed effects were driven by SEPs roughly occurring during the N and P waves of the VP, as the only comparisons surviving space-time permutation were bins #2 versus #4 (left, bins highlighted in orange; $t = 3.41$; $p = 0.0012$, electrode P4; cluster $t = 2,607.76$; cluster $p = 0.040$) and bins #2 versus #5 (left, bins highlighted in blue; $t = 3.39$; $p = 0.0012$, electrode P4; cluster $t = 2,946.37$; cluster $p = 0.032$). The results of t tests between all possible bin pairs are superimposed as gray thin waveforms, while the t tests for bins #2 versus #4 and #2 versus #5 are shown as colored, thicker waveforms. Specifically, SEP amplitude in the time interval corresponding to the P45 component was smaller in bin #2 compared with bins #4 and #5. Scalpmaps of the space-time corrected clusters at the latency of their highest t value (i.e., at 44 ms) are shown to the right. Note that the bins highlighted in orange and blue reflect the occurrence of the P45 component rather than the stimulus onset.

2. In a final analysis, we explored how the modulation of the P45 unfolded by extracting the timecourse of its amplitude throughout the concomitant VP. P45 amplitude broadly followed the shape of the VP: it decreased during the peak of the N wave, returned to the baseline at the transition between the N and P waves, became largest during the P wave, and decreased again after the VP (Fig. 4). This was substantiated by one-way ANOVA and subsequent *t* tests: There was strong evidence of P45 amplitude modulation across the entire VP waveform ($F_{(4,17, 91,83)} = 4.46; p = 0.0021$; one-way ANOVA), and post hoc *t* tests showed clear evidence that this effect was mostly driven by differences between the amplitude of P45 occurring during the N and the P waves (N peak vs P peak, $p = 0.0104$; N peak vs P end, $p = 0.0025$; Fig. 4). Importantly, the observed direction of P45 modulation was robust with respect to the time window chosen to extract the P45 amplitude. Indeed, this effect was also observed when the P45 amplitude was extracted from three additional wider time windows (Fig. S2).

When this P45 modulation timecourse was extracted from the “control SEP” waveforms (i.e., those generated using the “dummy VP phase binning”), the data were compatible with the null hypothesis of no difference of P45 amplitude across six bins ($F_{(3,97, 87,54)} = 0.93; p = 0.4464$; one-way ANOVA; Fig. S4).

A last control analysis showed that this VP phase-dependent modulation was only found for the P45 component. Indeed, we found no evidence of a difference of amplitude across time bins in the prestimulus ($F_{(4,30, 95,28)} = 1.86; p = 0.1185$; one-way

ANOVA) or at the end of the epoch ($F_{(3,76, 82,82)} = 1.59; p = 0.1869$; one-way ANOVA; Fig. S3).

Altogether, these results indicate that the S1 response at 45 ms poststimulus was tightly coupled to the phase of the concomitant auditory-evoked VP.

Discussion

In this work we tested the hypothesis that canonical lemniscal thalamocortical processing is modulated during a transient activation of the extralemniscal system. We activated the extralemniscal system using sudden and isolated auditory stimuli, while we continuously engaged the lemniscal system using a stream of somatosensory stimuli (Fig. 1).

We obtained three main results. (1) Lemniscal S1 responses occurring as early as 45 ms poststimulus are modulated when the extralemniscal system is activated. This change of S1 activity (2) reflects a modulation of lemniscal input at the cortical rather than subcortical level and (3) consists of an inhibition followed by an enhancement of lemniscal processing, aligned with the phase of the concomitant VP indexing the extralemniscal activation. In the light of previous empirical findings, these results demonstrate that a transient activation of the extralemniscal system modulates ongoing cortical function across different brain systems, i.e., not only at the motor output but already at the sensory input.

S1 responses to lemniscal input are modulated during a transient activation of the extralemniscal system

We first explored the cortical responsiveness to lemniscal somatosensory input during extralemniscal activation using a data-driven

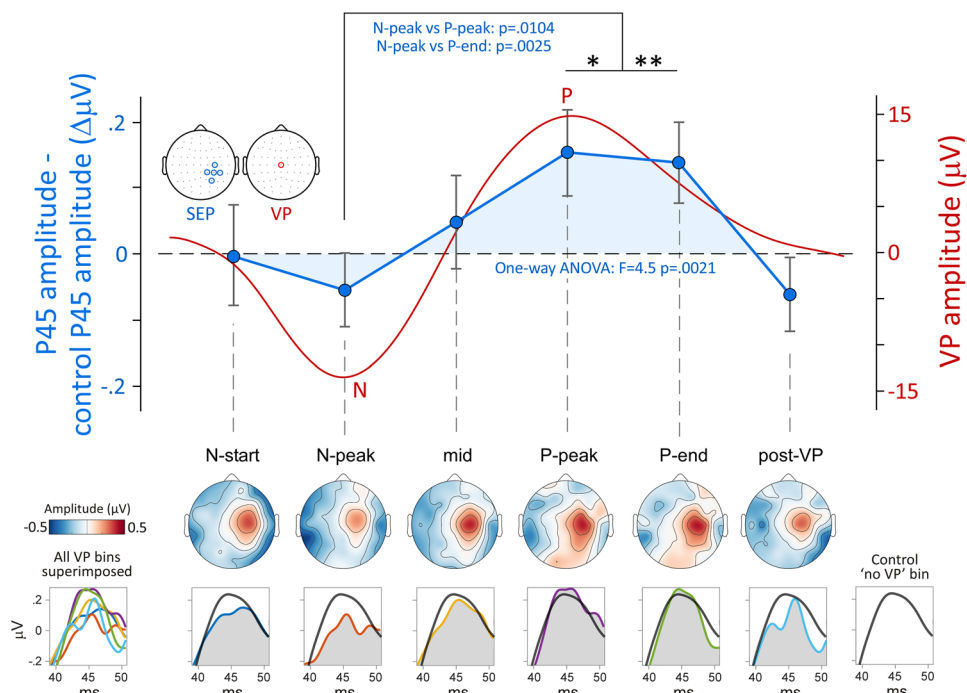


Figure 4. P45 amplitude reveals a phase-dependent modulation of S1 responsiveness. On the basis of the data-driven analysis on the entire SEP timecourse, we then focused on the P45 component, and extracted its amplitude for each time bin of the single-trial VP phase binning waveforms, in each subject. The top panel shows the change in P45 amplitude in each bin (blue) compared with P45 amplitude in the absence of the concomitant VP, together with the VP timecourse (red). One-way ANOVA revealed a dependence of P45 amplitude on the time bin ($F_{(4,17, 91,83)} = 4.46; p = 0.0021$). This effect was driven by a consistent amplitude difference when the P45 occurred during the N peak compared with both the P peak and the last part of the P wave (N peak vs P peak, $p = 0.0104$; N peak vs P end, $p = 0.0025$). The bottom panel shows group-level P45 waveforms (colored plots), together with the scalp maps in the 42–45 ms time window, and superimposed group-level P45 waveforms in the absence of the concomitant VP (gray plots). Note that the contralateral P45 somatosensory response decreases during the N and increases during the P wave.

approach that does not make assumptions about the temporal and spatial location of possible effects (Mouraux and Iannetti, 2008).

We found strong evidence that S1 activity changed depending on when it was sampled with respect to the onset of the auditory stimulus (Fig. 3, left panel). This observation suggested that S1 activity was dependent on the phase of the concomitant VP.

Before discussing the physiological implications of this modulation of lemniscal processing, it is important to consider that this result could have been consequent to two other explanations alternative to an effect of the extralemniscal activities indexed by the VP. In the two control analyses discussed in the next paragraph, we tested these alternatives.

The modulation of S1 lemniscal processing is tightly coupled to single-trial VP phase

The large latency jitter of the VP (Hu et al., 2011; Kilintari et al., 2018) allowed us to test if the modulation of lemniscal processing in S1 was due to processes independent of the VP but triggered by the same auditory stimulus. To this end, we examined the precise coupling between the modulation of SEP amplitude and the phase of the single-trial VP triggered by the same auditory stimulus. Specifically, we assigned SEP responses to bins on the basis of where the somatosensory stimulus landed as a function of the latency of the concomitant single-trial VP (Fig. 3, top panel). This analysis demonstrated that the S1 modulation was tightly linked to single-trial VP dynamics.

Still, we could not rule out that ongoing fluctuations of cortical excitability independent of the occurrence of the surprising stimulus that engaged the extralemniscal system were responsible for the observed modulation. Indeed, the phase of ongoing delta oscillations reflects increased cortical spiking and modulates subsequent stimulus processing (Schroeder and Lakatos, 2009; Whittingstall and Logothetis, 2009). Given that the frequency of the VP overlaps with the delta range (0.5–4 Hz; Mouraux et al., 2013), the algorithm for estimating the phase of individual VP waveforms applied to spontaneous EEG will necessarily detect one local minimum and one local maximum. In this second control analysis, we assigned somatosensory stimuli to bins based on the EEG minima and maxima identified in the spontaneous EEG. In this case, there was no evidence of a modulation of S1 activity in response to lemniscal input (Fig. S1).

Changes of S1 activity reflect a modulation of lemniscal input at the cortical rather than subcortical level

All these analyses indicated that the modulation of S1 activity in response to lemniscal input occurred ~45 ms poststimulus, with a scalp topography corresponding to the P45 SEP wave (Desmedt and Bourguet, 1985). In contrast, the earlier N20 wave, which reflects the first arrival of the lemniscal input to the cortex (Nuerer et al., 1994), was unaffected by the VP (Fig. 3). While an amplitude change of all SEP waves would have been compatible with a modulation at both the thalamic and cortical level, the lack of evidence of change during the N20 and P25 waves is consistent with a transient modulation of the S1 responses to lemniscal somatosensory input at the cortical level, rather than its gating at the thalamic level.

An alternative explanation is that, compared with the N20, the P45 reflects the activity of a larger neuronal population (Desmedt and Bourguet, 1985) and is therefore more amenable to display amplitude changes as a function of the cortical responsiveness and attentional state (Joshiassen et al., 1982; García-Larrea et al., 1991; Noguchi et al., 1995).

The transient activation of the extralemniscal system results in a rapid shift of cortical excitability

We found that S1 activity occurring 45 ms poststimulus followed a rapid biphasic pattern, coherent with the shift of VP polarity. Specifically, the P45 component was reduced during the negative VP deflection, started to increase at its negative-to-positive transition, and became largest during the positive VP deflection (Fig. 4).

This rapid alternation of periods of depressed and enhanced cortical excitability (Figs. 4, 5) is reminiscent of what occurs during the large, spontaneous slow waves of non-REM sleep (Massimini et al., 2003). Indeed, sleep slow waves are associated, at the neuronal level, with a short period of membrane hyperpolarization (cortical downstate) during which thalamocortical neurons stop firing for a few hundred milliseconds. This initial hyperpolarization is followed by a period of membrane depolarization (cortical upstate), during which neurons are more likely to fire (Steriade et al., 1993).

Interestingly, when probed during non-REM sleep, lemniscal somatosensory processing is affected by the phase of spontaneous slow waves (Massimini et al., 2003). Although the earliest S1 response (N20 wave) is already modulated by the concomitant slow waves, later components—such as the P60, which is the sleep equivalent of the P45 in wakefulness—are more profoundly affected (see Fig. 5 in Massimini et al., 2003). This is reminiscent of our observed modulation of the late P45 component. The difference between the SEP components affected in sleep and wakefulness is likely consequent to the fact that slow waves reflect more extreme fluctuations of neural excitability than those reflected by the VP (Compte et al., 2003). Therefore, our results provide evidence that the VP indexes a similar succession of down- and up states in wakefulness. Although this has yet to be conclusively demonstrated at the cellular level, a number of observations from invasive recording suggest this to be the case (Iurilli et al., 2012).

Thus, the transient activation of the extralemniscal system and its scalp manifestation as a large VP may reflect the activity of a diffuse thalamocortical neuromodulatory pathway similar to that mediating sleep slow waves.

Behavioral significance of the transient disruption of ongoing cortical processing

The bidirectional effect of VP phase on lemniscal sensory processing adds to a wealth of evidence that a transient activation of the extralemniscal system by sudden, isolated, and unexpected sensory stimuli modulates ongoing cortical function at large, from early sensory input to motor output. This modulation consistently manifests as an inhibition followed by an enhancement of ongoing cortical activity. Figure 5 provides examples of such modulations across different brain systems.

For example, in primates, the corticospinal drive subserving the execution of an isometric force task is reduced during the negative and enhanced during the positive VP wave (Novembre et al., 2018, 2019, 2024; Somervail et al., 2022). A similar alternation of inhibition and enhancement of motor output is observed across a range of tasks (Novembre and Iannetti, 2021).

This inhibition–excitation sequence of cortical activity seems to occur consistently across different types of motor output (Fig. 5). For instance, when auditory and visual stimuli appropriate to engage the extralemniscal system are delivered during a fixation task, the rate of spontaneous microsaccades is initially suppressed and then rapidly enhanced before returning to the

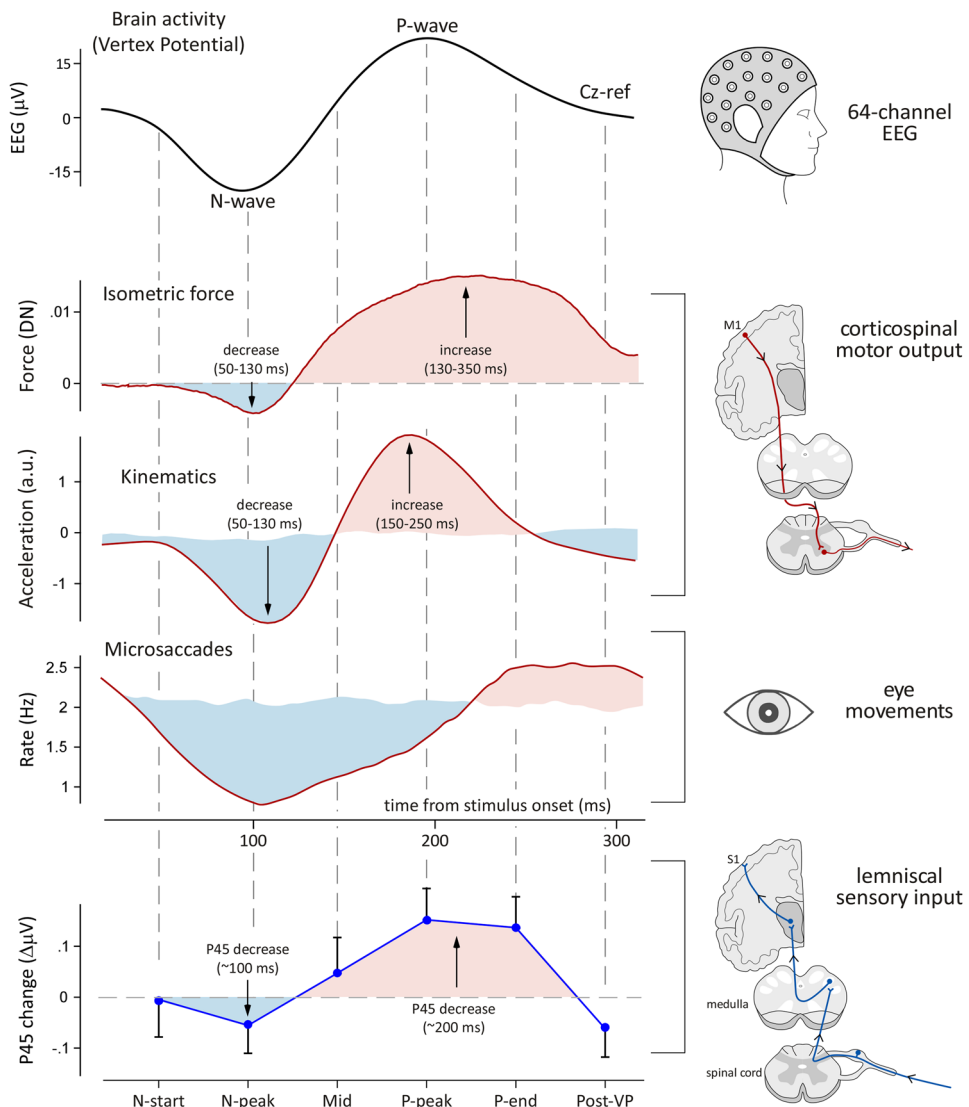


Figure 5. Generality of the extralemniscal effects on ongoing cortical activity. Isolated and unexpected sensory stimuli engage the extralemniscal system and elicit large-amplitude and long-latency widespread negative–positive potentials, maximal at the vertex (VP, top row). The extralemniscal activation modulates ongoing cortical function across a number of functional domains, taking the form of an inhibition followed by an enhancement of ongoing cortical activity, tightly coupled to the negative and positive VP waves. This bipolar modulation is observed when the corticospinal system is engaged in isometric force and kinematic tasks (second and third rows; adapted from Novembre et al., 2018), in saccades and microsaccades (fourth row; the apparent lower frequency of the modulation of the microsaccade rate is likely due to the 100 ms moving window used to compute it; Engbert and Kliegl, 2003). The present work shows that the transient activation of the extralemniscal system similarly modulates early processing of lemniscal input in the primary somatosensory cortex, in the form of an inhibition-enhancement of the amplitude of P45 somatosensory-evoked component (bottom row).

baseline (Engbert and Kliegl, 2003; Rolfs et al., 2008). The current results show that a transient extralemniscal activation also affects the very first cortical handling of somatosensory input (Nuwer et al., 1994), demonstrating the generality of the effects of extralemniscal activity on brain dynamics.

Whether these effects are epiphenomenal or reflect a functionally significant “cortical reset” that interrupts and overrides ongoing brain function remains an open issue. This rapid shift in cortical excitability could make the system better at reacting rapidly immediately after the occurrence of a surprising stimulus. Results of experiments exploring the relationship between VP amplitude and the more effective execution of urgent behaviors remain conflicting (Moayedi et al., 2015; Kilintari et al., 2018). Still, these observations suggest that the rapid switch between two cortical excitability microstates indexed by the VP has the

capacity to provide a behavioral benefit when an agent needs to react swiftly to environmental changes.

References

- Abrahamian HA, Allison T, Goff WR, Rosner BS (1963) Effects of thiopental on human cerebral evoked responses. *Anesthesiology* 24:650–657.
- Albe-Fessard D, Besson JM (1973) Somatosensory system. In: *Handbook of sensory physiology* (Iggo A, ed), pp 489–560. Berlin, Heidelberg: Springer-Verlag.
- Albe-Fessard D, Rougeul A (1958) Activités d'origine somesthésique évoquées sur le cortex non-spécifique du chat anesthésié au chloralose: Rôle du centre médian du thalamus. *Electroencephalogr Clin Neurophysiol* 10:131–152.
- Baker SN, Gabriel C, Lemon RN (2003) EEG oscillations at 600Hz are macroscopic markers for cortical spike bursts. *J Physiol* 550:529–534.
- Bancaud J, Bloch V, Paillard J (1953) Contribution EEG; à l'étude des potentiels évoqués chez l'homme au niveau du vertex. *Rev Neurol* 89:399–418.

- Clynes M (1969) Dynamics of vertex evoked potentials: the R-M brain function. In: *Average evoked potentials: methods, results, and evaluations* (Donchin E, Lindsley DB, eds), pp 363–374. San Francisco: US National Aeronautics and Space Administration.
- Compte A, Sanchez-Vives MV, McCormick DA, Wang XJ (2003) Cellular and network mechanisms of slow oscillatory activity (<1Hz) and wave propagations in a cortical network model. *J Neurophysiol* 89: 2707–2725.
- Cruciu G, Aminoff MJ, Curio G, Guerit JM, Kakigi R, Mauguire F, Rossini PM, Treede RD, Garcia-Larrea L (2008) Recommendations for the clinical use of somatosensory-evoked potentials. *Clin Neurophysiol* 119:1705–1719.
- Davis H, Davis PA, Loomis AL, Harvey EN, Hobart G (1939) Electrical reactions of the human brain to auditory stimulation during sleep. *J Neurophysiol* 2:500–514.
- Desmedt JE, Huy NT, Bourguet M (1983) The cognitive P40, N60 and P100 components of somatosensory evoked potentials and the earliest electrical signs of sensory processing in man. *Electroencephalogr Clin Neurophysiol* 56:272–282.
- Desmedt JE, Bourguet M (1985) Color imaging of parietal and frontal somatosensory potential fields evoked by stimulation of median or posterior tibial nerve in man. *Electroencephalogr Clin Neurophysiol* 62:1–17.
- Engbert R, Kliegl R (2003) Microsaccades uncover the orientation of covert attention. *Vision Res* 43:1035–1045.
- Garcia-Larrea L, Bastuji H, Mauguire F (1991) Mapping study of somatosensory evoked potentials during selective spatial attention. *Electroencephalogr Clin Neurophysiol* 80:201–214.
- Gastaut HJ, Benoit PH, Vigouroux M, Roger A (1954) Potentiels évoqués par des stimuli auditifs sur la région temporelle de certains épileptiques. *Electroencephalogr Clin Neurophysiol* 6:557–564.
- Hu B (2003) Functional organization of lemniscal and nonlemniscal auditory thalamus. *Exp Brain Res* 153:543–549.
- Hu L, Mouraux A, Hu Y, Iannetti GD (2010) A novel approach for enhancing the signal-to-noise ratio and detecting automatically event-related potentials (ERPs) in single trials. *Neuroimage* 50:99–111.
- Hu L, Liang M, Mouraux A, Wise RG, Hu Y, Iannetti GD (2011) Taking into account latency, amplitude, and morphology: improved estimation of single-trial ERPs by wavelet filtering and multiple linear regression. *J Neurophysiol* 106:3216–3229.
- Iannetti GD, Hughes NP, Lee MC, Mouraux A (2008) Determinants of laser-evoked EEG responses: pain perception or stimulus saliency? *J Neurophysiol* 100:815–828.
- Iurilli G, Ghezzi D, Olcese U, Lassi G, Nazzaro C, Tonini R, Tucci V, Benfenati F, Medini P (2012) Sound-driven synaptic inhibition in primary visual cortex. *Neuron* 73:814–828.
- Josiasen RC, Shagass C, Roemer RA, Ercegovac DV, Straumanis JJ (1982) Somatosensory evoked potential changes with a selective attention task. *Psychophysiology* 19:146–159.
- Jung TP, Makeig S, Humphries C, Lee TW, McKeown MJ, Iragui V, Sejnowski TJ (2000) Removing electroencephalographic artifacts by blind source separation. *Psychophysiology* 37:163–178.
- Kerzel D, Born S, Souto D (2010) Inhibition of steady-state smooth pursuit and catch-up saccades by abrupt visual and auditory onsets. *J Neurophysiol* 104:2573–2585.
- Kilintari M, Bufacchi RJ, Novembre G, Guo Y, Haggard P, Iannetti GD (2018) High-precision voluntary movements are largely independent of preceding vertex potentials elicited by sudden sensory events: event-related potentials and subsequent voluntary movements. *J Physiol* 596:3655–3673.
- Komura Y, Tamura R, Uwano T, Nishijo H, Ono T (2005) Auditory thalamus integrates visual inputs into behavioral gains. *Nat Neurosci* 8:1203–1209.
- Lemus L, Hernández A, Luna R, Zainos A, Romo R (2010) Do sensory cortices process more than one sensory modality during perceptual judgments? *Neuron* 67:335–348.
- Maris E, Oostenveld R (2007) Nonparametric statistical testing of EEG-and MEG-data. *J Neurosci Methods* 164:177–190.
- Massimini M, Rosanova M, Mariotti M (2003) EEG slow (~1Hz) waves are associated with nonstationarity of thalamo-cortical sensory processing in the sleeping human. *J Neurophysiol* 89:1205–1213.
- Moayed M, Liang M, Sim AL, Hu L, Haggard P, Iannetti GD (2015) Laser-evoked vertex potentials predict defensive motor actions. *Cereb Cortex* 25:4789–4798.
- Moruzzi G, Magoun HW (1949) Brain stem reticular formation and activation of the EEG. *Electroencephalogr Clin Neurophysiol* 1:455–473.
- Mountcastle VB (1974) *Medical physiology*. St. Louis, MO: CV Mosby.
- Mountcastle VB (2005) *The sensory hand: neural mechanisms of somatic sensation*. Cambridge, Massachusetts: Harvard University Press.
- Mouraux A, Iannetti GD (2008) Across-trial averaging of event-related EEG responses and beyond. *Magn Reson Imaging* 26:1041–1054.
- Mouraux A, Iannetti GD (2009) Nociceptive laser-evoked brain potentials do not reflect nociceptive-specific neural activity. *J Neurophysiol* 101:3258–3269.
- Mouraux A, De Paepe AL, Marot E, Plaghki L, Iannetti GD, Legrain V (2013) Unmasking the obligatory components of nociceptive event-related brain potentials. *J Neurophysiol* 110:2312–2324.
- Noguchi Y, Yamada T, Yeh M, Matsubara M, Kokubun Y, Kawada J, Shiraishi G, Kajimoto S (1995) Dissociated changes of frontal and parietal somatosensory evoked potentials in sleep. *Neurology* 45:154–160.
- Novembre G, Iannetti GD (2021) Towards a unified neural mechanism for reactive adaptive behaviour. *Prog Neurobiol* 204:102115.
- Novembre G, Pawar VM, Bufacchi RJ, Kilintari M, Srinivasan M, Rothwell JC, Haggard P, Iannetti GD (2018) Saliency detection as a reactive process: unexpected sensory events evoke corticomuscular coupling. *J Neurosci* 38:2385–2397.
- Novembre G, Pawar VM, Kilintari M, Bufacchi RJ, Guo Y, Rothwell JC, Iannetti GD (2019) The effect of salient stimuli on neural oscillations, isometric force, and their coupling. *Neuroimage* 198:221–230.
- Novembre G, Lacal I, Benusiglio D, Quarta E, Schito A, Grasso S, Caratelli L, Caminiti R, Mayer AB, Iannetti GD (2024) A cortical mechanism linking saliency detection and motor reactivity in rhesus monkeys. *J Neurosci* 44: 1–10.
- Nuwer MR, Aminoff M, Desmedt J, Eisen AA, Goodin D, Matsuoka S, Mauguire F, Shibasaki H, Sutherling W, Vibert JF (1994) IFCN recommended standards for short latency somatosensory evoked potentials. Report of an IFCN committee. *Electroencephalogr Clin Neurophysiol* 91:6–11.
- Peacocke C (2015) Perception and the first person. In: *The oxford handbook of the philosophy of perception* (Mohan M, ed), pp 168–180. Oxford: Oxford University Press.
- Rolfs M, Kliegl R, Engbert R (2008) Toward a model of microsaccade generation: the case of microsaccadic inhibition. *J Vis* 8:5.
- Schroeder CE, Lakatos P (2009) Low-frequency neuronal oscillations as instruments of sensory selection. *Trends Neurosci* 32:9–18.
- Somervail R, Zhang F, Novembre G, Bufacchi RJ, Guo Y, Crepaldi M, Hu L, Iannetti GD (2021) Waves of change: brain sensitivity to differential, not absolute, stimulus intensity is conserved across humans and rats. *Cereb Cortex* 31:949–960.
- Somervail R, Bufacchi RJ, Salvatori C, Neary-Zajicsek L, Guo Y, Novembre G, Iannetti GD (2022) Brain responses to surprising stimulus offsets: phenomenology and functional significance. *Cereb Cortex* 32:2231–2244.
- Somervail R, Perovic S, Bufacchi RJ, Caminiti R, Iannetti GD (2025) A two-system theory of sensory-evoked brain responses. *Brain*, in press.
- Steriade M, McCormick DA, Sejnowski TJ (1993) Thalamocortical oscillations in the sleeping and aroused brain. *Science* 262:679–685.
- Whittingstall K, Logothetis NK (2009) Frequency-band coupling in surface EEG reflects spiking activity in monkey visual cortex. *Neuron* 64:281–289.